

Learning Aligned Cross-modal Representations for Referring Image Segmentation

Zhichao Wei¹Xiaohao Chen¹Mingqiang Chen¹Siyu Zhu¹¹Alibaba Group

Abstract

Referring image segmentation aims to segment the image region of interest according to the given language expression, which is a typical multi-modal task. One of the critical challenges of this task is to align semantic representations for different modalities including vision and language. To achieve this, previous methods perform cross-modal interactions to update visual features but ignore the role of integrating fine-grained visual features into linguistic features. We present **AlignFormer**, an end-to-end framework for referring image segmentation. Our AlignFormer views the linguistic feature as the center embedding and segments the region of interest by pixels grouping based on the center embedding. For achieving the pixel-text alignment, we design a **Vision-Language Bidirectional Attention module (VLBA)** and resort contrastive learning. Concretely, the VLBA enhances visual features by propagating semantic text representations to each pixel and promotes linguistic features by fusing fine-grained image features. Moreover, we introduce the cross-modal instance contrastive loss to alleviate the influence of pixel samples in ambiguous regions and improve the ability to align multi-modal representations. Extensive experiments demonstrate that our AlignFormer achieves a new state-of-the-art performance on RefCOCO, RefCOCO+, and RefCOCOg by large margins.

1. Introduction

Referring image segmentation aims to generate a segmentation mask for the target object corresponding to a given text description. In contrast to traditional segmentation tasks [11–13, 28] which can only process a predefined set of categories, referring image segmentation is no longer limited to specific classes and has wider applications including human-robot interaction [37] and interactive photo editing [3].

Although recent deep-learning-based methods have achieved remarkable performance in this area, referring image segmentation is still a challenging task. The first challenge is that vision and language modality naturally main-

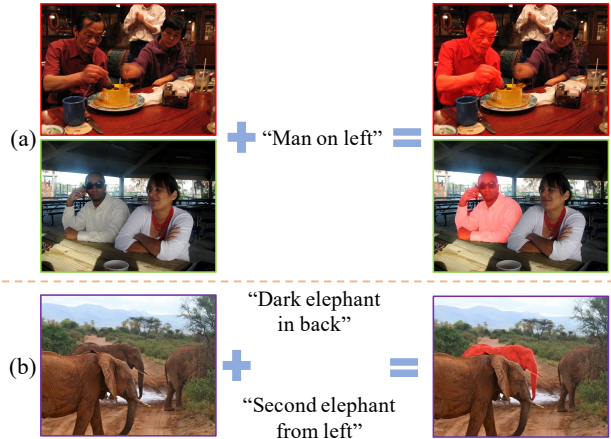


Figure 1. Illustration of the variety of images and languages. (a) shows that the same language may be associated with different images. (b) shows that the same image may be associated with different languages.

tain different attributes, aligning pixel-level visual features to corresponding holistic linguistic features is difficult. Another challenge is the variety of images and languages. The same language expression associated with different images yields completely different segmentation results, while different language expressions related to the same image produce the same segmentation results, as shown in Fig. 1.

Based on the design principles, existing methods for referring image segmentation can be divided into two categories namely decoder-fusion and encoder-fusion, as shown in Fig. 2. Previous methods [2, 8, 15–17, 22, 25, 26, 32, 38, 39, 43] often employ the decoder-fusion strategy, which first extracts visual and linguistic features from two independent uni-modal encoders respectively, then fuses these cross-modal representations into the same embedding space and finally generates the target mask. Decoder-fusion methods only interact with high-level features of two modalities and miss the importance of low-level visual features such as texture, shape, and color, as well as word features. Some recent works [10, 23, 41] proposed encoder-fusion methods to solve the referring image segmentation problem. These methods perform cross-modal interactions on visual and linguistic

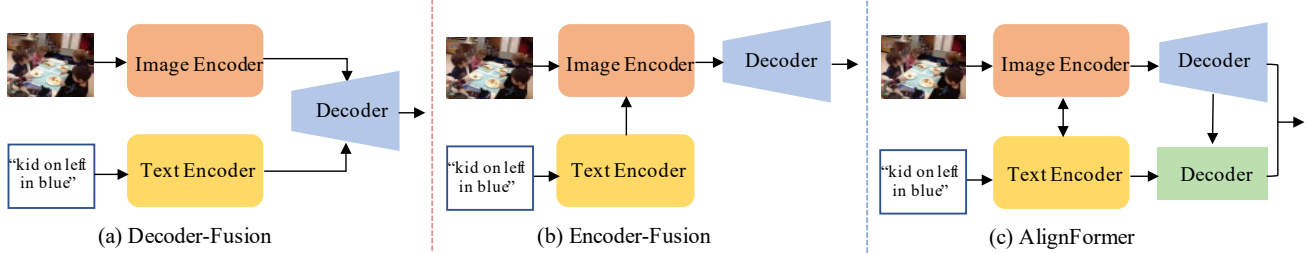


Figure 2. Illustration of the main architectures for referring image segmentation. (a) The decoder-fusion-based framework. (b) The encoder-fusion-based framework. (c) Our proposed AlignFormer framework.

features in the early encoder stage to update visual features. Both decoder-fusion methods and encoder-fusion methods were focused on aggregating linguistic features into visual features to obtain text-aligned visual features but neglected the role of aligning linguistic features with visual features. We believe this scheme is insufficient to simultaneously address the inconsistency and variety of cross-modal input.

As shown in Fig. 2(c), we propose AlignFormer, an end-to-end framework for referring image segmentation that first introduces updating visual-attended linguistic features as well as linguistic-attended visual features simultaneously for better cross-modal representations alignment. Inspired by recent query-based mask transformer methods [5, 6], our AlignFormer treats linguistic features as the center embedding and segments objects by grouping pixel features according to the center embedding. Our experiments demonstrate that this framework is more conducive for aligning cross-modal representations, as it explicitly introduces cross-modal representations alignment and optimizes both linguistic features and visual features simultaneously. For vision-language encoding, we design a vision-language bidirectional attention module (VLBA) that promotes visual features and linguistic features simultaneously by propagating semantic text representations to per-pixel features and enhancing linguistic features by fusing fine-grained visual features. For vision-language decoding, a pixel decoder is employed to integrate multi-scale visual features, and then use a transformer decoder to align linguistic features with visual features. Moreover, we introduce cross-modal instance contrastive learning to alleviate the influence of pixel samples in ambiguous regions whose labels are likely to be inaccurate and facilitate better alignment of cross-modal features.

To summarize, our main contributions are as follows:

- We propose AlignFormer, a transformer-based method that first introduces updating visual-attended linguistic features as well as linguistic-attended visual features simultaneously for better cross-modal representations alignment.
- The proposed method achieves new state-of-the-art results on multiple datasets without bells and whistles,

demonstrating the effectiveness of our method.

2. Related Work

Referring Image Segmentation. Early works mainly focused on fusing multi-modal representations on the decoder. Hu *et al.* [14] proposed to utilize CNN and RNN to extract visual and linguistic features separately and then obtain a segmentation mask through the concatenation-convolution operation. Based on this pipeline, some works [2, 15, 25, 42] improved the performance by utilizing more powerful feature encoders and designing more ingenious fusion strategies (*e.g.*, recurrent fusion). With the success of attention mechanisms in the communities of natural language processing and computer vision, follow-up works [8, 21, 29, 43] attempted to model intra-modal and cross-modal relationships by adopting self-attention and cross-attention operations. For example, Ye *et al.* [43] proposed Cross-Modal Self-Attention (CMSA) to highlight informative visual and linguistic elements. Ding *et al.* [8] used vision-guided attention to generate multiple linguistic queries which understand language expression from different aspects. Kim *et al.* [21] conducted both intra-modality and inter-modality interactions by self-attention operations, alleviating the weakness of CNN in capturing language information and cross-modal information.

Recent studies [10, 19, 41] have shown that cross-modal interactions during feature extraction can further enhance multi-modal alignment. Feng *et al.* [10] replaced the vision encoder with a multi-modal encoder by adopting an early cross-modal interaction strategy, which achieved deep interweaving between visual and linguistic features. Yang *et al.* [41] adopted language-aware visual attention during feature encoding and effectively exploited the transformer encoder for modeling multi-modal context.

The method most related to ours is CRIS [38], where the transformer encodes linguistic and visual features separately, then aggregates cross-modal features at the decoder, and finally performs text-to-pixel contrastive learning to align cross-modal features.

Compared to CRIS [38], we obtain the center embedding for text-to-pixel contrastive learning by cross-modal

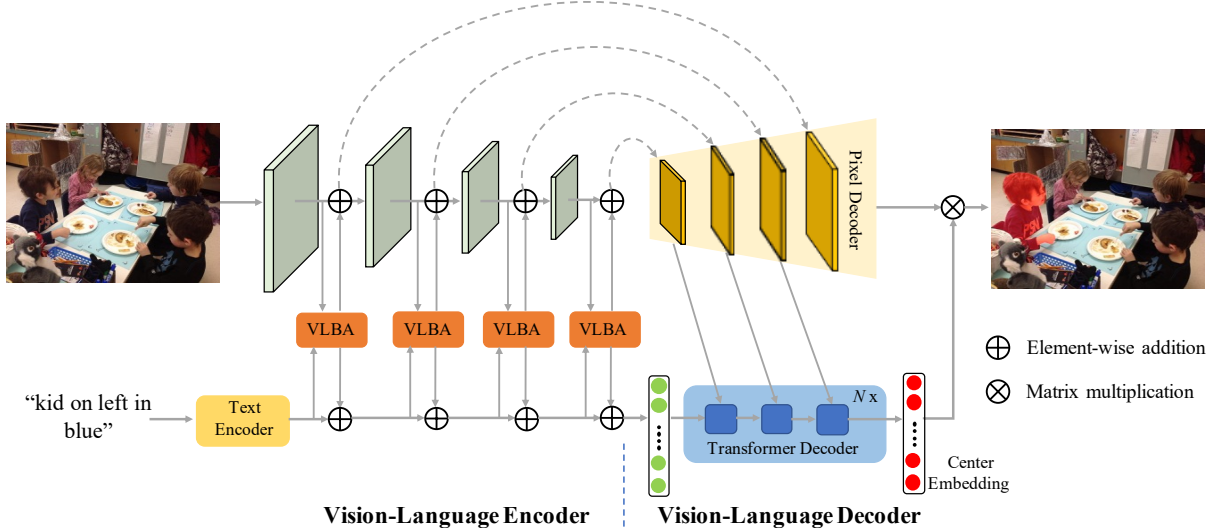


Figure 3. An overview of the AlignFormer framework. It consists of a vision-language encoder with our proposed VLBA module for cross-modal interactions, a vision-language decoder with a pixel decoder for integrating multi-scale visual features, and a transformer decoder for generating the visual-attended linguistic features as the center embedding.

interactions at the encoder and decoder rather than directly extracting by a language encoder. Moreover, we propose a cross-modal instance contrastive loss to alleviate the influence of pixel samples in ambiguous regions. Our method can achieve a better cross-modal alignment without contrastive language-image pretraining (CLIP) [33].

Transformers for Segmentation. With the long-range modeling ability of the attention mechanism, the transformer architecture has dominated most computer vision tasks, such as image classification [9, 27, 36] and object detection [1, 46].

Some segmentation works [5, 6, 35, 45] also employed transformers with additional cross-attention as mask decoder which generates segmentation masks by object queries (*i.e.*, learnable embeddings). Wang *et al.* [35] proposed an end-to-end panoptic segmentation method named Max-DeepLab which employs a mask decoder to generate dynamic filters.

Cheng *et al.* [6] proposed MaskFormer which shows well performance in both semantic- and instance-level segmentation tasks in a unified manner. By using mask attention, multi-scale high-resolution features, and optimizing the training strategy, Mask2Former [5] outperformed specialized architectures across different segmentation tasks by a universal image segmentation architecture. From the perspective of clustering, Yu *et al.* [45] proposed kMax-DeepLab, endowing better interpretation ability of mask decoder. Inspired by these works, we extend this paradigm into referring image segmentation by treating vision-attended linguistic features as queries and achieving

cross-modal alignment.

3. Method

In this section, we first overview two frameworks commonly used in traditional image segmentation tasks, including the per-pixel classification framework and query-based mask transformer framework, and describe how we extend the latter to referring image segmentation task. Then, we introduce the network structure and details of the proposed AlignFormer. Finally, we describe how we perform the vision-language contrastive learning for better cross-modal alignment.

3.1. Cross-modal Representations Grouping

Per-pixel Classification Prototype Inspired by traditional semantic segmentation methods, most of the existing referring image segmentation methods adopt the per-pixel classification framework to generate the segmentation mask by using a linear classifier (*i.e.*, a fully connected layer) to assign each pixel a semantic label $\hat{y}_i \in \{1, \dots, K\}$, where i is the pixel index and K is the total category number.

Cross-modal Representations Grouping Prototype Different from the per-pixel classification framework, the recent query-based mask transformer framework groups pixels into non-overlapping segments by predicting a set of binary masks with corresponding labels. These masks are generated by the dot product between pixel features and center embeddings (also known as object queries) which aggregate information about different

objects through transformer decoders. By defining labels with different semantics (*e.g.*, categories or instances), the query-based mask transformer framework can be used for both semantic- and instance-level segmentation tasks.

Our AlignFormer also adopts this paradigm, but additionally considers language modality. Specifically, to extend this framework into referring image segmentation task, we view visual-attended linguistic features as the center embedding and update it with linguistic-attended visual features continuously through transformer decoders. The pixels will be grouped into different segments (*i.e.*, the referred image region and background) based on their similarities to the center embedding.

3.2. Architecture

As illustrated in Fig. 3, the proposed AlignFormer takes an image and a language expression as input and outputs a mask for the region of interest. Firstly, the input image and expression are transformed into multi-modal features through visual-language joint encoding, which leverages the proposed VLBA for early cross-modal alignment. Secondly, the multi-scale linguistic-attended visual features are fed into the pixel decoder to generate more fine-grained semantic representations. Then, the multi-scale visual features from the pixel decoder are sent to the transformer decoder together with the linguistic features to obtain visual-attended linguistic features as the center embedding. Finally, the mask is obtained by the dot product between the visual-attended linguistic features (*i.e.*, the center embedding) from the transformer decoder and the linguistic-attended visual features refined by the pixel decoder.

Vision-Language Encoder For the input image and language expression, we adopt a deep hierarchical vision model (*e.g.*, Swin Transformer [27]) to extract multi-scale visual features and a deep language model to extract linguistic features, respectively. Specially, we introduce a vision-language joint encoding strategy for early cross-modal alignment, which is achieved by the proposed VLBA along each stage of the visual encoder.

Vision-Language Bidirectional Attention Module To segment the image region described by the language expression, it is important to well align visual and linguistic representations. For achieving this, recent studies have designed various attention-based cross-modal interaction modules, but they all tend to view linguistic information as supplements and use linguistic features to update visual features unidirectionally. Unlike previous methods, we believe that linguistic information is equally important as visual information for referring image segmentation, and visual features should be deeply intertwined with linguistic features to achieve better alignment. Therefore, we design

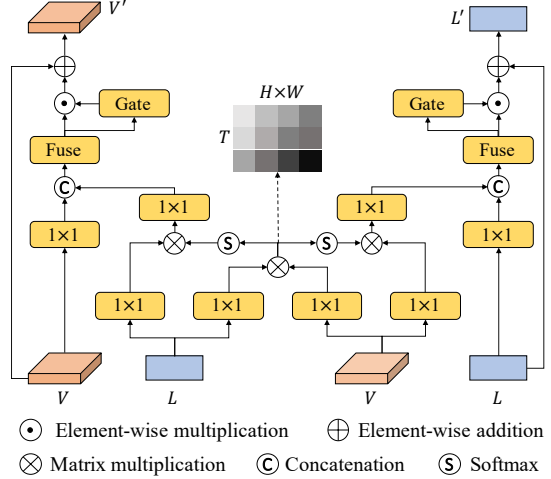


Figure 4. The detailed process of our proposed visual-language bidirectional attention (VLBA) module with a symmetric structure. The module takes linguistic features L and visual features V as input and updates them mutually.

the vision-language bidirectional attention module (**VLBA**) with a symmetric structure to update visual and linguistic features mutually.

As shown in Fig. 4, the proposed VLBA module takes the visual features $V \in \mathbb{R}^{H \times W \times C_v}$ and the linguistic features $L \in \mathbb{R}^{T \times C_l}$ from the last stage as input, and update them mutually through two operations, *i.e.*, bidirectional cross-attention and feature fusion, where H , W , C_v , T and C_l are the height, width, channels of the visual feature maps, the word length and the channels of linguistic feature maps.

First, cross-attention is employed to aggregate relevant cross-modal information according to the similarities of visual and linguistic features. Specifically, the responses of each location of visual feature maps aggregate relevant linguistic information across word dimensions, and the responses of each location of linguistic feature maps aggregate relevant visual information across spatial pixel dimensions. To improve the computational efficiency, instead of performing two cross-attention operations to update the visual and linguistic features separately, we update the features of the two modalities mutually through a single cross-attention operation by sharing the attention map. Concretely, the responses of visual and linguistic features are obtained as follows:

$$A = \frac{V_q L_k^T}{\sqrt{C_v}} \quad (1)$$

$$V_r = w_1 \left(\underset{T}{\text{softmax}}(A) L_v \right) \quad (2)$$

$$L_r = w_2 \left(\underset{HW}{\text{softmax}}(A^T) V_v \right) \quad (3)$$

where V_q and V_v are the query embeddings and value embeddings of V . L_k and L_v are the key embeddings and value embeddings of L . w_1 and w_2 represent linear projections. V_r and L_r are the responses of visual features and linguistic features obtained from each other. $\text{softmax}(\cdot)$ and $\text{softmax}(\cdot)$ means to normalize the attention map along different dimensions, *i.e.*, word dimension or spatial pixel dimension. By sharing the attention map, the unidirectional cross-attention is converted into the bidirectional cross-attention, thereby realizing the mutual flow of visual and linguistic information.

Second, the responses V_r and L_r will be fused into the input visual and linguistic features in the form of residuals to avoid interference caused by irrelevant compensation information. This process is formulated as:

$$V_m = \text{fuse}(\text{cat}(V, V_r)) \quad (4)$$

$$L_m = \text{fuse}(\text{cat}(L, L_r)) \quad (5)$$

$$V' = V + V_m \odot \text{gate}(V_m) \quad (6)$$

$$L' = L + L_m \odot \text{gate}(L_m) \quad (7)$$

where \odot denotes element-wise multiplication. Both $\text{fuse}(\cdot)$ and $\text{gate}(\cdot)$ are implemented as a two-layer MLP, where $\text{fuse}(\cdot)$ is used to fuse the original features and its responses from the other modality, and $\text{gate}(\cdot)$ is used to weight the fused features to generate adaptive residuals.

Vision-Language Decoder The cross-modal decoder of our AlignFormer consists of two components: pixel decoder and transformer decoder. The pixel decoder is used to enhance per-pixel feature representations and gradually recover the spatial resolution. The transformer decoder extracts global information from the multi-scale features produced by the pixel decoder to update the center embedding, enabling further cross-modal alignment. The segmentation mask is generated based on the similarities of per-pixel features to the center embedding.

Following [5], we employ multi-scale deformable transformer [46] as the pixel decoder to obtain finer features. Specifically, the feature maps with resolution 1/8, 1/16, and 1/32 from the encoder are fed into 6 deformable transformer layers, and the bilinear interpolation is applied to the feature map with resolution 1/8 to generate the feature maps with resolution 1/4 which is used to obtain the segmentation mask.

Our transformer decoder consists of 6 naive transformer decoder layers [34], with the center embedding generated by the language expression as query and multi-scale features from pixel decoder with resolution 1/8, 1/16 and 1/32 as key and value. The query num is 1 as there is only one referred image region. The multi-scale strategy [5] is adopted

to improve model performance for segmenting objects of different scales.

3.3. Vision-Language Contrastive Learning

Most of the existing methods are based on the per-pixel classification framework which performs feature alignment implicitly. In contrast, our pixel grouping-based approach can easily introduce contrastive learning for explicit feature alignment, thus achieving better segmentation results.

Pixel-Text Contrastive Learning We introduce the contrastive loss to explicitly align visual and linguistic features. Given the center embedding (visual-attended linguistic features) $L_e \in \mathbb{R}^{C_e}$ from transformer decoder and per-pixel embeddings (linguistic-attended visual features) $V_e \in \mathbb{R}^{N_e \times C_e}$ from pixel decoder, the pixel-text contrastive loss is formulated as:

$$\mathcal{L}_{pt}^i = \begin{cases} -\log \sigma((L_e \cdot V_e^i)) & \text{if } y^i = 1 \\ -\log(1 - \sigma((L_e \cdot V_e^i))) & \text{otherwise} \end{cases} \quad (8)$$

$$\mathcal{L}_{pt} = \frac{1}{N_e} \sum_{i=1}^{N_e} \mathcal{L}_{pt}^i(L_e, V_e^i) \quad (9)$$

where $\sigma(\cdot)$ is the sigmoid function. N_e and C_e are the spatial size and channels of the visual feature maps V_e . $y^i \in \{0, 1\}$ and V_e^i are the ground truth label and the per-pixel embeddings at the i -th position of V_e .

The contrastive loss pulls the center embedding to all pixel embeddings in the region of interest and pushes the center embedding away from all pixel embeddings of the background. However, this strategy treats all pixel embeddings equally and ignores the problem of label errors in ambiguous regions (regions where labels are likely to be inaccurate, such as object boundary regions), leading to unexpected center embedding shifts, as depicted in Fig. 5. The ideal center embedding should be approximately in the center of all positive pixel embeddings and away from negative pixel embeddings.

However, the labels of pixel samples in ambiguous regions are unreliable. According to Eq. (8), pixel samples with incorrect labels would move the center embedding away from the ideal position and results in poor segmentation results.

Cross-modal Instance Contrastive Learning To get a more proper center embedding, we propose Cross-Modal Instance Contrastive (CMIC) Loss, which performs better cross-modal feature alignment by weakening the importance of false negatives (FNs) and false positives (FPs) to the center embedding. The core idea behind this is that FNs

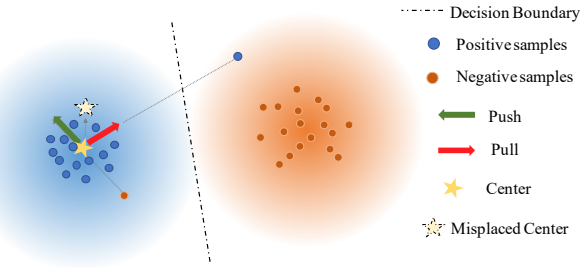


Figure 5. The pixel-text contrastive loss treats pixels in ambiguous regions as important as others, resulting in unexpected shifts for the center embedding.

and FPs often exist in ambiguous regions, both of which could lead to unexpected center embedding shifts.

As depicted in Eq. (11) and Eq. (10), for each false negative, it is pulled toward M randomly selected true positives (TPs) in addition to the center embedding, and for each false positive, it is pulled toward M randomly selected true negatives (TNs) in addition to being pushed away from the center embedding. The Cross-Modal Instance Contrastive Loss is formulated as:

$$\mathcal{L}_{cmic}^{fp} = -\frac{1}{N_{fp}} \sum_{i=1}^{N_{fp}} \sum_{j=1}^M \lambda_j^{fp} \log \sigma(V_{ei}^{fp} \cdot V_{ej}^{tn}) \quad (10)$$

$$\mathcal{L}_{cmic}^{fn} = -\frac{1}{N_{fn}} \sum_{i=1}^{N_{fn}} \sum_{j=1}^M \lambda_j^{fn} \log \sigma(V_{ei}^{fn} \cdot V_{ej}^{tp}) \quad (11)$$

$$\mathcal{L}_{cmic}(L_e, V_e) = \mathcal{L}_{cmic}^{fp} + \mathcal{L}_{cmic}^{fn} \quad (12)$$

where $\lambda_j^{fp} = 1 - \sigma(L_e \cdot V_{ej}^{tn})$ and $\lambda_j^{fn} = \sigma(L_e \cdot V_{ej}^{tp})$, V_e^{fp} , V_e^{tn} , V_e^{fn} and V_e^{tp} denote false positives, true negatives, false negatives and true positives visual embeddings respectively. N_{fp} and N_{fn} represent the number of false positive pixels and false negative pixels.

With the CMIC loss, the negative effects caused by pixels in ambiguous regions do not act totally on the linguistic center embedding but spread over the linguistic center embedding and other selected visual embeddings, which can alleviate the unexpected shifts of the center embedding. What's more, this strategy is equivalent to providing a soft center embedding for each misclassified pixel embedding, which can preserve the cross-modal alignment ability for misclassified pixels.

Finally, the total loss of AlignFormer is as follows:

$$\mathcal{L}_{total}(L_e, V_e) = \mathcal{L}_{pt}(L_e, V_e) + \lambda \mathcal{L}_{cmic}(L_e, V_e) \quad (13)$$

where λ is a constant used to balance the cross-modal instance contrastive loss.

4. Experiments

4.1. Experimental Setup

Datasets and Metrics RefCOCO [20] and RefCOCO+ [20] are the two largest and most commonly used referring image segmentation datasets in existing open-source data. The RefCOCO dataset contains 19,994 images and 142,209 language expressions to describe 50,000 segmented object regions. These data were selected from the MS COCO dataset [24] by a two-player game. In general, each image contains multiple objects of the same class, and the average length of each expression is 3.5 words. It is divided into a training set with 120,624 samples, a validation set with 10,834 samples, a test set A with 5,657 samples, and a test set B with 5,095 samples. The RefCOCO+ dataset contains 26,711 images and 104,560 language expressions to describe 54,822 segmented object regions. It is divided into a training set with 120,191 samples, a validation set with 10,758 samples, a test set A with 5,726 samples, and a test set B with 4,889 samples. Unlike RefCOCO, expressions in RefCOCO+ contain more occurrences than absolute positions. The RefCOCOg dataset [31], collected from MSCOCO via Amazon's Mechanical Turk, consists of 104,560 expressions involving 54,822 objects in 26,711 images. Unlike RefCOCO, it is longer at 8.4 words, including the appearance and location of the referent, which makes the dataset particularly challenging.

We adopt three metrics to verify the effectiveness: overall intersection-over-union (oIoU), mean intersection-over-union (mIoU), and *Precision@X*. The oIoU metric measures the ratio of the total intersection area and union area between the predicted mask and the ground truth for all samples under test. The mIoU is used to evaluate the average overlap ratio between the predicted and ground truth. *Precision@X* is used to measure the percentage of the IoU score of the predicted mask in the test set that exceeds the set threshold X , in this paper $X \in \{0.5, 0.7, 0.9\}$.

Implementation Details We utilize PyTorch to implement our method. The vision and language encoders use Swin Transformer [27] and BERT [7] respectively, and their initialization parameters are from the official pre-trained model. To make a fair comparison with the state-of-the-art methods, we use the *Swin-base* as the vision backbone and the *bert-base-uncased* as the language model. To facilitate experiments, we use the *Swin-small* as the vision model in the ablation study. All other parameters in the network are initialized randomly. For optimization, we adopt the AdamW optimizer with a weight decay of 0.01 and an initial learning rate of 5e-5. All input images are resized to 480×480 and no additional data augmentation is applied. We train the model for 40 epochs, and the training batch size is fixed at 32. We empirically set $M = 20$ and $\lambda = 0.5$.

| Method | RefCOCO | | | RefCOCO+ | | | RefCOCOg | | |
|-------------------|--------------|--------------|--------------|--------------|--------------|--------------|--------------|--------------|--------------|
| | val | testA | testB | val | testA | testB | val(U) | test(U) | val(G) |
| DMN [32] | 49.78 | 54.83 | 45.13 | 38.88 | 44.22 | 32.29 | - | - | 36.76 |
| RRN [22] | 55.33 | 57.26 | 53.93 | 39.75 | 42.15 | 36.11 | - | - | 36.45 |
| MAttNet [44] | 56.51 | 62.37 | 51.70 | 46.67 | 52.39 | 40.08 | 47.64 | 48.61 | - |
| CMSA [43] | 58.32 | 60.61 | 55.09 | 43.76 | 47.60 | 37.89 | - | - | 39.98 |
| CAC [4] | 58.90 | 61.77 | 53.81 | - | - | - | 46.37 | 46.95 | 44.32 |
| STEP [2] | 60.04 | 63.46 | 57.97 | 48.19 | 52.33 | 40.41 | - | - | 46.40 |
| BRINet [15] | 60.98 | 62.99 | 59.21 | 48.17 | 52.32 | 42.11 | - | - | 48.04 |
| CMPC [16] | 61.36 | 64.53 | 59.64 | 49.56 | 53.44 | 43.23 | - | - | 49.05 |
| LSCM [17] | 61.47 | 64.99 | 59.55 | 49.34 | 53.12 | 43.50 | - | - | 48.05 |
| CMPC+ [26] | 62.47 | 65.08 | 60.82 | 50.25 | 54.04 | 43.47 | - | - | 49.89 |
| MCN [30] | 62.44 | 64.20 | 59.71 | 50.62 | 54.99 | 44.69 | 49.22 | 49.40 | - |
| EFN [10] | 62.76 | 65.69 | 59.67 | 51.50 | 55.24 | 43.01 | - | - | 51.93 |
| BUSNet [40] | 63.27 | 66.41 | 61.39 | 51.76 | 56.87 | 44.13 | - | - | 50.56 |
| CGAN [29] | 64.86 | 68.04 | 62.07 | 51.03 | 55.51 | 44.06 | 51.01 | 51.69 | 46.54 |
| LTS [18] | 65.43 | 67.76 | 63.08 | 54.21 | 58.32 | 48.02 | 54.40 | 54.25 | - |
| VLT [8] | 65.65 | 68.29 | 62.73 | 55.50 | 59.20 | 49.36 | 52.99 | 56.65 | 49.76 |
| CRIS [38] | 70.47 | 73.18 | 66.10 | 62.27 | 68.08 | 53.68 | 59.87 | 60.36 | - |
| LAVT [41] | 72.73 | 75.82 | 68.79 | 62.14 | 68.38 | 55.10 | 61.24 | 62.09 | 60.50 |
| AlignFormer(ours) | 73.73 | 77.00 | 70.64 | 64.55 | 70.19 | 56.18 | 63.56 | 64.83 | 62.12 |

Table 1. Comparison with state-of-the-art methods.

4.2. Comparison with State-of-the-art

In Tab. 1, we compare our proposed AlignFormer with previous state-of-the-art methods on three widely used referring image segmentation datasets, detailed in Sec. 4.1. As can be seen from the Tab. 1, our method outperforms other methods on all datasets.

On the RefCOCO dataset, the oIoU of the proposed method is at least 1% higher than the best comparison method LAVT [41]. Furthermore, on the more complex and difficult dataset RefCOCO+, our method still achieves a performance gain of more than 1%, especially on the val split, which is nearly 2.4%. On RefCOCOg, another dataset with a longer average length of language expressions, our method also outperforms other methods by 1% at least on each split set. These results show that our method is more expressive in difficult cases. We believe this is because long and complex sentences usually contain more information and our proposed AlignFormer can better extract linguistic information and achieve visual and linguistic alignment.

In Fig. 6, we visualize some segmentation results on the RefCOCO val set.

4.3. Ablation Study

Effect of Cross-modal Representations Grouping To verify the effectiveness of the cross-modal grouping framework in the referring image segmentation task, we compare it with the per-pixel classification method, as shown in Tab. 2. For the per-pixel classification framework, we remove the transformer decoder and add a linear classifier to

| Method | split | P@0.5 | P@0.7 | P@0.9 | oIoU | mIoU |
|--------------------------|-------|-------|-------|-------|-------|-------|
| Per-pixel Classification | val | 83.48 | 73.47 | 31.65 | 70.74 | 72.97 |
| | testA | 86.95 | 78.08 | 32.35 | 74.75 | 75.81 |
| | testB | 77.51 | 65.65 | 32.40 | 65.96 | 68.83 |
| Cross-modal Grouping | val | 84.93 | 76.09 | 33.00 | 72.04 | 74.15 |
| | testA | 87.59 | 79.34 | 33.46 | 75.34 | 76.31 |
| | testB | 79.51 | 69.05 | 33.84 | 68.68 | 70.88 |

Table 2. Comparison of the results of the per-pixel classification and the cross-modal representations grouping.

| Method | split | P@0.5 | P@0.7 | P@0.9 | oIoU | mIoU |
|------------------------------|-------|-------|-------|-------|-------|-------|
| w/o cross-modal interactions | val | 30.13 | 17.08 | 2.28 | 32.74 | 30.83 |
| | testA | 34.06 | 20.28 | 2.51 | 34.70 | 33.18 |
| | testB | 31.71 | 19.47 | 2.62 | 33.19 | 31.66 |
| VLUA | val | 84.75 | 75.90 | 32.58 | 71.70 | 74.05 |
| | testA | 87.45 | 79.30 | 33.20 | 74.32 | 76.09 |
| | testB | 78.14 | 67.81 | 33.68 | 66.85 | 69.79 |
| VLBA | val | 84.93 | 76.09 | 33.00 | 72.04 | 74.15 |
| | testA | 87.59 | 79.34 | 33.46 | 75.34 | 76.31 |
| | testB | 79.51 | 69.05 | 33.84 | 68.68 | 70.88 |

Table 3. The VLBA module consistently improves the network performance on referring image segmentation, showing that VLBA is effective and stable on multiple RefCOCO test sets.

output per-pixel class scores as segmentation results. Almost all the results of the cross-modal grouping are 1% higher than the framework based on the per-pixel classification on different test sets. Especially in the testB split,

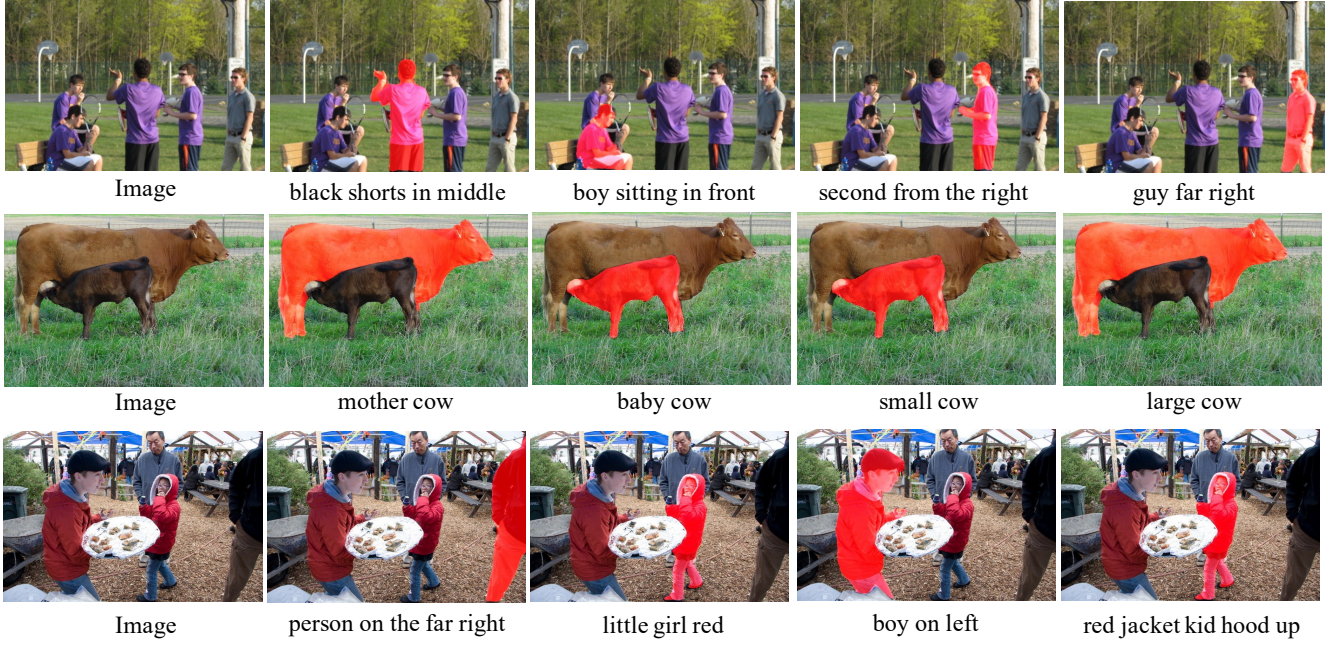


Figure 6. Visualization examples of AlignFormer on the RefCOCO val set.

the oIOU is nearly 2.7% higher. These results demonstrate the advantage of cross-modal representations grouping for cross-modal alignment, as it explicitly introduces pixel-text contrastive learning.

Effect of Vision-Language Bidirectional Attention In Tab. 3, we evaluate the importance of cross-modal interactions in the vision-language encoder. As a baseline, the visual and linguistic features are extracted separately without cross-modal interactions, then the vision-language decoder and cross-modal representations grouping are performed. Tab. 3 shows that the performance of adopting cross-modal grouping without cross-modal interactions declines significantly. To verify the effect of promoting visual features and linguistic features simultaneously, we design a Vision-to-Language Unidirectional Attention module(VLUA) by removing the vision-to-language attention in the VLBA, which means the linguistic features are not fused with visual features in the vision-language encoder. From the Tab. 3, we can see that the VLBA can consistently improve the network performance on all the RefCOCO test sets. The effective and stable performance of VLBA demonstrates that promoting the multi-modal features simultaneously can better perform the cross-modal alignment.

Effect of Cross-modal Instance Contrastive Learning By weakening the importance of pixel embeddings in ambiguous regions, we introduce additional CMIC loss to obtain more appropriate center embedding. To further study

| Method | split | P@0.5 | P@0.7 | P@0.9 | oIoU | mIoU |
|-------------------|-------|-------|-------|-------|-------|-------|
| w/o CMIC Loss | val | 83.70 | 74.22 | 32.26 | 71.09 | 73.29 |
| | testA | 87.06 | 78.01 | 32.44 | 74.24 | 75.66 |
| | testB | 78.55 | 68.81 | 34.15 | 66.98 | 70.07 |
| with CMIC Loss | val | 84.93 | 76.09 | 33.00 | 72.04 | 74.15 |
| | testA | 87.59 | 79.34 | 33.46 | 75.34 | 76.31 |
| | testB | 79.51 | 69.05 | 33.84 | 68.68 | 70.88 |

Table 4. Ablation on CMIC Loss on the RefCOCO dataset.

the relative contribution of this loss to the AlignFormer, we conducted experiments on RefCOCO data, as shown in Tab. 4. The results display that introducing CMIC Loss can achieve higher performance. Compared with utilizing pixel-text contrastive learning only, introducing the CMIC Loss can perform a more robust cross-modal feature alignment.

5. Conclusion

In this paper, we propose AlignFormer for referring image segmentation. In addition, to achieve better pixel-text alignment, we design the vision-language bidirectional attention (VLBA) module. Moreover, the cross-modal instance contrastive (CMIC) loss is equipped to reduce the impact of pixel samples in ambiguous regions and improve the ability to align multi-modal representations. Extensive experiments show that the proposed method is superior to the previous state-of-the-art methods in performance.

References

- [1] Nicolas Carion, Francisco Massa, Gabriel Synnaeve, Nicolas Usunier, Alexander Kirillov, and Sergey Zagoruyko. End-to-end object detection with transformers. In *European Conference on Computer Vision (ECCV)*, 2020. 3
- [2] Ding-Jie Chen, Songhao Jia, Yi-Chen Lo, Hwann-Tzong Chen, and Tyng-Luh Liu. See-through-text grouping for referring image segmentation. In *International Conference on Computer Vision (ICCV)*, 2019. 1, 2, 7
- [3] Jianbo Chen, Yelong Shen, Jianfeng Gao, Jingjing Liu, and Xiaodong Liu. Language-based image editing with recurrent attentive models. In *Conference on Computer Vision and Pattern Recognition (CVPR)*, 2018. 1
- [4] Yi-Wen Chen, Yi-Hsuan Tsai, Tiantian Wang, Yen-Yu Lin, and Ming-Hsuan Yang. Referring expression object segmentation with caption-aware consistency. *arXiv preprint arXiv:1910.04748*, 2019. 7
- [5] Bowen Cheng, Ishan Misra, Alexander G Schwing, Alexander Kirillov, and Rohit Girdhar. Masked-attention mask transformer for universal image segmentation. In *Conference on Computer Vision and Pattern Recognition (CVPR)*, 2022. 2, 3, 5
- [6] Bowen Cheng, Alex Schwing, and Alexander Kirillov. Per-pixel classification is not all you need for semantic segmentation. *Advances in Neural Information Processing Systems (NIPS)*, 2021. 2, 3
- [7] Jacob Devlin, Ming-Wei Chang, Kenton Lee, and Kristina Toutanova. Bert: Pre-training of deep bidirectional transformers for language understanding. *arXiv preprint arXiv:1810.04805*, 2018. 6
- [8] Henghui Ding, Chang Liu, Suchen Wang, and Xudong Jiang. Vision-language transformer and query generation for referring segmentation. In *International Conference on Computer Vision (ICCV)*, 2021. 1, 2, 7
- [9] Alexey Dosovitskiy, Lucas Beyer, Alexander Kolesnikov, Dirk Weissenborn, Xiaohua Zhai, Thomas Unterthiner, Mostafa Dehghani, Matthias Minderer, Georg Heigold, Sylvain Gelly, et al. An image is worth 16x16 words: Transformers for image recognition at scale. *arXiv preprint arXiv:2010.11929*, 2020. 3
- [10] Guang Feng, Zhiwei Hu, Lihe Zhang, and Huchuan Lu. Encoder fusion network with co-attention embedding for referring image segmentation. In *Conference on Computer Vision and Pattern Recognition (CVPR)*, 2021. 1, 2, 7
- [11] Jun Fu, Jing Liu, Haijie Tian, Yong Li, Yongjun Bao, Zhiwei Fang, and Hanqing Lu. Dual attention network for scene segmentation. In *Conference on Computer Vision and Pattern Recognition (CVPR)*, 2019. 1
- [12] Junjun He, Zhongying Deng, Lei Zhou, Yali Wang, and Yu Qiao. Adaptive pyramid context network for semantic segmentation. In *Conference on Computer Vision and Pattern Recognition (CVPR)*, 2019. 1
- [13] Kaiming He, Georgia Gkioxari, Piotr Dollár, and Ross Girshick. Mask r-cnn. In *International Conference on Computer Vision (ICCV)*, 2017. 1
- [14] Ronghang Hu, Marcus Rohrbach, and Trevor Darrell. Segmentation from natural language expressions. In *European Conference on Computer Vision (ECCV)*, 2016. 2
- [15] Zhiwei Hu, Guang Feng, Jiayu Sun, Lihe Zhang, and Huchuan Lu. Bi-directional relationship inferring network for referring image segmentation. In *Conference on Computer Vision and Pattern Recognition (CVPR)*, 2020. 1, 2, 7
- [16] Shaofei Huang, Tianrui Hui, Si Liu, Guanbin Li, Yunchao Wei, Jizhong Han, Luoqi Liu, and Bo Li. Referring image segmentation via cross-modal progressive comprehension. In *Conference on Computer Vision and Pattern Recognition (CVPR)*, 2020. 1, 7
- [17] Tianrui Hui, Si Liu, Shaofei Huang, Guanbin Li, Sansi Yu, Fuxi Zhang, and Jizhong Han. Linguistic structure guided context modeling for referring image segmentation. In *European Conference on Computer Vision (ECCV)*, 2020. 1, 7
- [18] Ya Jing, Tao Kong, Wei Wang, Liang Wang, Lei Li, and Tieniu Tan. Locate then segment: A strong pipeline for referring image segmentation. In *Conference on Computer Vision and Pattern Recognition (CVPR)*, 2021. 7
- [19] Aishwarya Kamath, Mannat Singh, Yann LeCun, Gabriel Synnaeve, Ishan Misra, and Nicolas Carion. Mdet-modulated detection for end-to-end multi-modal understanding. In *International Conference on Computer Vision (ICCV)*, 2021. 2
- [20] Sahar Kazemzadeh, Vicente Ordonez, Mark Matten, and Tamara Berg. Referitgame: Referring to objects in photographs of natural scenes. In *Conference on Empirical Methods in Natural Language Processing (EMNLP)*, 2014. 6
- [21] Namyup Kim, Dongwon Kim, Cuiling Lan, Wenjun Zeng, and Suha Kwak. Restr: Convolution-free referring image segmentation using transformers. In *Conference on Computer Vision and Pattern Recognition (CVPR)*, 2022. 2
- [22] Ruiyu Li, Kaican Li, Yi-Chun Kuo, Michelle Shu, Xiaojuan Qi, Xiaoyong Shen, and Jiaya Jia. Referring image segmentation via recurrent refinement networks. In *Conference on Computer Vision and Pattern Recognition (CVPR)*, 2018. 1, 7
- [23] Zizhang Li, Mengmeng Wang, Jianbiao Mei, and Yong Liu. Mail: A unified mask-image-language trimodal network for referring image segmentation. *arXiv preprint arXiv:2111.10747*, 2021. 1
- [24] Tsung-Yi Lin, Michael Maire, Serge Belongie, James Hays, Pietro Perona, Deva Ramanan, Piotr Dollár, and C Lawrence Zitnick. Microsoft coco: Common objects in context. In *European Conference On Computer Vision (ECCV)*, 2014. 6
- [25] Chenxi Liu, Zhe Lin, Xiaohui Shen, Jimei Yang, Xin Lu, and Alan Yuille. Recurrent multimodal interaction for referring image segmentation. In *International Conference on Computer Vision (ICCV)*, 2017. 1, 2
- [26] Si Liu, Tianrui Hui, Shaofei Huang, Yunchao Wei, Bo Li, and Guanbin Li. Cross-modal progressive comprehension for referring segmentation. *Pattern Analysis and Machine Intelligence (PAMI)*, 2021. 1, 7

- [27] Ze Liu, Yutong Lin, Yue Cao, Han Hu, Yixuan Wei, Zheng Zhang, Stephen Lin, and Baining Guo. Swin transformer: Hierarchical vision transformer using shifted windows. In *International Conference on Computer Vision (ICCV)*, 2021. 3, 4, 6
- [28] Jonathan Long, Evan Shelhamer, and Trevor Darrell. Fully convolutional networks for semantic segmentation. In *Conference on Computer Vision and Pattern Recognition (CVPR)*, 2015. 1
- [29] Gen Luo, Yiyi Zhou, Rongrong Ji, Xiaoshuai Sun, Jinsong Su, Chia-Wen Lin, and Qi Tian. Cascade grouped attention network for referring expression segmentation. In *ACM International Conference on Multimedia (ACM MM)*, 2020. 2, 7
- [30] Gen Luo, Yiyi Zhou, Xiaoshuai Sun, Liujuan Cao, Chenglin Wu, Cheng Deng, and Rongrong Ji. Multi-task collaborative network for joint referring expression comprehension and segmentation. In *Conference on Computer Vision and Pattern Recognition (CVPR)*, 2020. 7
- [31] Junhua Mao, Jonathan Huang, Alexander Toshev, Oana Camburu, Alan L Yuille, and Kevin Murphy. Generation and comprehension of unambiguous object descriptions. In *Conference on Computer Vision and Pattern Recognition (CVPR)*, 2016. 6
- [32] Edgar Margffoy-Tuay, Juan C Pérez, Emilio Botero, and Pablo Arbeláez. Dynamic multimodal instance segmentation guided by natural language queries. In *European Conference on Computer Vision (ECCV)*, 2018. 1, 7
- [33] Alec Radford, Jong Wook Kim, Chris Hallacy, Aditya Ramesh, Gabriel Goh, Sandhini Agarwal, Girish Sastry, Amanda Askell, Pamela Mishkin, Jack Clark, et al. Learning transferable visual models from natural language supervision. In *International Conference on Machine Learning (ICML)*, 2021. 3
- [34] Ashish Vaswani, Noam Shazeer, Niki Parmar, Jakob Uszkoreit, Llion Jones, Aidan N Gomez, Łukasz Kaiser, and Illia Polosukhin. Attention is all you need. *Advances in Neural Information Processing Systems (NIPS)*, 2017. 5
- [35] Huiyu Wang, Yukun Zhu, Hartwig Adam, Alan Yuille, and Liang-Chieh Chen. Max-deeplab: End-to-end panoptic segmentation with mask transformers. In *Conference on Computer Vision and Pattern Recognition (CVPR)*, 2021. 3
- [36] Wenhui Wang, Enze Xie, Xiang Li, Deng-Ping Fan, Kaitao Song, Ding Liang, Tong Lu, Ping Luo, and Ling Shao. Pyramid vision transformer: A versatile backbone for dense prediction without convolutions. In *International Conference on Computer Vision (ICCV)*, 2021. 3
- [37] Xin Wang, Qiuyuan Huang, Asli Celikyilmaz, Jianfeng Gao, Dinghan Shen, Yuan-Fang Wang, William Yang Wang, and Lei Zhang. Reinforced cross-modal matching and self-supervised imitation learning for vision-language navigation. In *Conference on Computer Vision and Pattern Recognition (CVPR)*, 2019. 1
- [38] Zhaoqing Wang, Yu Lu, Qiang Li, Xunjiang Tao, Yandong Guo, Mingming Gong, and Tongliang Liu. Cris: Clip-driven referring image segmentation. In *Conference on Computer Vision and Pattern Recognition (CVPR)*, 2022. 1, 2, 7
- [39] Jianzong Wu, Xiangtai Li, Xia Li, Henghui Ding, Yunhai Tong, and Dacheng Tao. Towards robust referring image segmentation. *arXiv preprint arXiv:2209.09554*, 2022. 1
- [40] Sibei Yang, Meng Xia, Guanbin Li, Hong-Yu Zhou, and Yizhou Yu. Bottom-up shift and reasoning for referring image segmentation. In *Conference on Computer Vision and Pattern Recognition (CVPR)*, 2021. 7
- [41] Zhao Yang, Jiaqi Wang, Yansong Tang, Kai Chen, Hengshuang Zhao, and Philip HS Torr. Lavt: Language-aware vision transformer for referring image segmentation. In *Conference on Computer Vision and Pattern Recognition (CVPR)*, 2022. 1, 2, 7
- [42] Linwei Ye, Zhi Liu, and Yang Wang. Dual convolutional lstm network for referring image segmentation. *IEEE Transactions on Multimedia*, 2020. 2
- [43] Linwei Ye, Mrigank Rochan, Zhi Liu, and Yang Wang. Cross-modal self-attention network for referring image segmentation. In *Conference on Computer Vision and Pattern Recognition (CVPR)*, 2019. 1, 2, 7
- [44] Licheng Yu, Zhe Lin, Xiaohui Shen, Jimei Yang, Xin Lu, Mohit Bansal, and Tamara L Berg. Mattnet: Modular attention network for referring expression comprehension. In *Conference on Computer Vision and Pattern Recognition (CVPR)*, 2018. 7
- [45] Qihang Yu, Huiyu Wang, Siyuan Qiao, Maxwell Collins, Yukun Zhu, Hartwig Adam, Alan Yuille, and Liang-Chieh Chen. k-means mask transformer. In *European Conference on Computer Vision (ECCV)*, 2022. 3
- [46] Xizhou Zhu, Weijie Su, Lewei Lu, Bin Li, Xiaogang Wang, and Jifeng Dai. Deformable detr: Deformable transformers for end-to-end object detection. *arXiv preprint arXiv:2010.04159*, 2020. 3, 5